Supplementary Material (ESI) for Analyst.
This journal is © The Royal Society of Chemistry 2016

Electronic Supplementary Information (ESI) available for:

Microfluidic Array for Simultaneous Detection of DNA Oxidation and DNA-Adduct Damage

Boya Song, [ς] Min Shen, [ς] Di Jiang, [ς] Spundana Malla, [ς] Islam M. Mosa, [ς,α] Dharamainder Choudhary[β] and James F. Rusling*[ς,β,γ]

[ς]Department of Chemistry and Institute of Materials Science, University of Connecticut, Storrs, CT, USA 06269.

α Department of Chemistry, Tanta University, Tanta, Egypt.

[β]Department of Surgery and Neag Cancer Center, University of Connecticut Health Center, Farmington, CT, USA 06032.

[γ]School of Chemistry, National University of Ireland, Galway.

Experimental Section

Chemicals and materials.

Polyguanylic acid potassium salt (polyG), deoxyguanosine (dG), 8-oxo-7-hydro-2'-deoxyguanosine (8-oxodG), and salmon testes (ST) ds-DNA (2000 base pairs av, 41.2% G/C), poly(diallyldimethylammonium chloride) (PDDA), poly-(sodium 4-styrenesulfonate) (PSS), $CuCl_2$, $MgCl_2$, dimethyl sulfoxide (DMSO), tetrahydrofuran (THF), 17β-estradiol (E_2), catechol, 2-nitrosotoluene (2-NO-T), 4-hydroxyestradiol (4-OHE_2), 2-hydroxyestradiol (2-OHE_2), 4-(Methylnitrosamino)-1-(3-pyridyl)-1-butanone (NNK), 2-acetylaminofluorene (2-AAF), D-glucose 6-phosphate sodium salt (G6P),β-nicotinamide adenine dinucleotide phosphate sodium salt hydrate ($NADP^+$), and glucose-6-phosphate dehydrogenase (G6PDH) were from Sigma-Aldrich (St. Louis, MO). Pooled male human liver microsomes (HLM, 20 mg mL^{-1} in 250 mM sucrose), Pooled male rat liver microsomes (RLM, 20 mg mL^{-1} in 250 mM sucrose) were purchased from Corning Gentest (Woburn, MA). Water was treated with a Hydro Nanopure system to specific resistance >16 mΩ cm.

Sensor array fabrication.

Metallopolymers/DNA/Enzyme films were formed as a thin film on the sensor element using 1 μL droplets of previously optimized solution compositions. Solutions were (a) PDDA, 2 mg mL^{-1} in 0.05 M NaCl; (b) PSS 3 mg mL^{-1} in 0.05 M NaCl; (c) OsPVP, 2.5 mg mL^{-1} in 50% V/V ethanol; (d) RuPVP, 2.5 mg mL^{-1} in 50% V/V ethanol; (e) ds-DNA, 2 mg mL^{-1} in 10 mM Tris + 0.5 M NaCl, pH 7.4; (d) human liver microsomes (HLM), 20 mg mL^{-1} in 250 mM sucrose. PDDA, PSS and metallopolymers adsorbate solution were sequentially incubated on the sensor element for 20 min, enzymes and DNA were incubated for 30 min at 4 °C, washing with water

between depositions. Preliminary studies employing different masses of DNA concluded that 22 ng was the best compromise between good signal to noise and conservation of sample size.

Microfluidic sensor device.

The microfluidic sensor consisted a molded polydimethylsiloxane (PDMS) slab with 60 µL rectangular microchannel, two pieces of hard poly-(methylmethacrylate) (PMMA) plates, and Ag/AgCl wire reference and a Pt wire counter electrode inserted in the top plate. These two wires were running along the full channel length. The array was sandwiched in between the PDMS slab and bottom PMMA plate to immobilize the 8 electrodes of the array in the center of the microchannel.

Film characterization.

Quartz Crystal Microbalance (QCM, USI Japan) with 9 MHz QCM quartz resonators (AT-cut, International Crystal Mfg. Company) was used to monitor the layer-by-layer assembling process. A negatively charged monolayer of 3-mercaptopropionic acid (MPA) was coated on the gold resonator (0.16 ± 0.01 cm^2) before film assembling. Then the same film fabrications as arrays were followed to deposit layers on the gold resonators. The frequency change for dried films was recorded at ambient temperature.

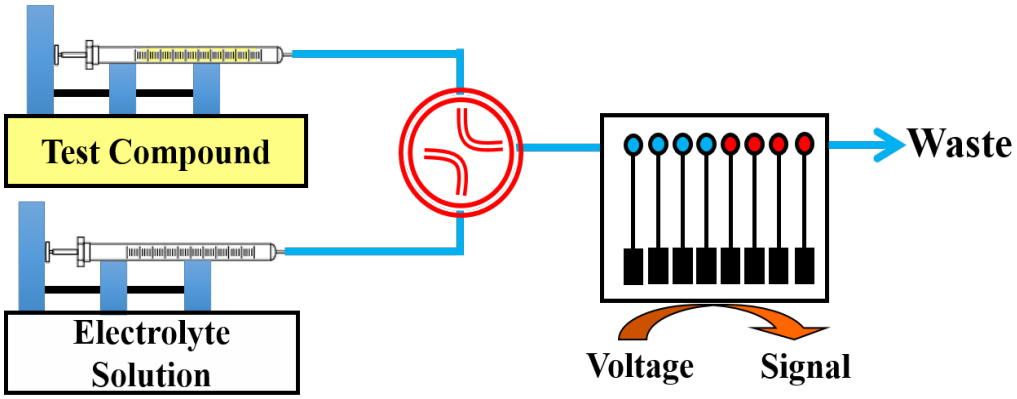

Scheme S1. Microfluidic array sensor for DNA-adduct and oxidation damage analysis. The microfluidic array device features a two-channel syringe pump and a switch valve connected in series to the inlet of the 8-sensor array.

Voltammetric analysis of both DNA damage by mixture of test compounds.

Two representative test compounds NNK and catechol, which were reported to form DNA adducts or form DNA oxidation, were mixed together to validate the ability of analysis of both DNA damage by the sensor. The reactant solution containing 150 µM NNK, 100 µM catechol, and 0.5 mM Cu^{2+}, NADPH regenerating system in pH 7.0 Tris buffer was pumped into the microfluidic c sensor coated with DNA, HLM and metallopolymers at a constant flow rate of 50 µL min^{-1} for different reaction intervals. A potential of -0.65 V vs Ag/AgCl was applied for up to 90 s, followed by continuously pumping of reactant solution. Afterwards, the microfluidic channel was flushed with acetate buffer for 2 min. The SWV were recorded (4 mV step; 25 mV

pulse; 15 Hz frequency) on all 8 electrodes by using an eight-channel CHI 1040b electrochemical workstation.

Voltammetric analysis of both DNA damage by cigarette smoke.

Cigarette smoke from a lit cigarette was collected by a syringe with a cotton plug. After trapping the smoke, the cotton plug was extracted with 100 μL of THF. The reactant solution containing 100-fold diluted cigarette smoke extract with pH 7 Tris buffer, 0.5 mM Cu^{2+} and NADPH regenerating system was pumped into the microfluidic sensor coated with DNA, HLM and metallopolymers at a constant flow rate of 50 μL min^{-1} for different reaction intervals. A potential of - 0.65 V vs Ag/AgCl was applied for up to 90 s, followed by continuously pumping of reactant solution. Afterwards, the microfluidic channel was flushed with acetate buffer for 2 min. The SWV were recorded (4 mV step; 25 mV pulse; 15 Hz frequency) on all 8 electrodes by using an eight-channel CHI 1040b electrochemical workstation.

Voltammetric analysis of DNA damage by parent compound

Rat liver microsomes (RLM) 300 μL (20 mg mL^{-1} in 250 mM sucrose), 1 mM E_2, NADPH regenerating system were incubated in pH 7 Tris buffer in a total volume of 3 mL for 30 min at 37 ºC. Reaction was terminated by extracting the metabolites by 1 mL ethyl acetate twice.[1] Extracts were combined, evaporated under vacuum, and reconstituted in 15 μL of DMSO. Fifteen microliter of extract was added in 3 mL pH 7 Tris buffer with 0.5 mM Cu^{2+} and NADPH regenerating system. This solution was pumped into the microfluidic channel at a constant flow rate of 50 μL min^{-1}. Then the microfluidic channel was washed with acetate buffer for 2 min, following SWV recording (4 mV step; 25 mV pulse; 15 Hz frequency) on the array.

UPLC-MS/MS detection of DNA damage.

The filtered sample solutions were diluted 10-fold with water and transferred into sample vials. Samples were analyzed using a Dionex Ultimate 3000 UHPLC system (Thermo Scientific, Dionex, Sunnyvale, California, USA), interfaced to an Applied Biosystems 4000 QTRAP triple quadrupole linear ion trap mass spectrometer (AB Sciex) equipped with an electrospray ionization source (ESI). Compounds were separated by a reversed phase analytical column (Thermo Scientific, Hypersil GOLD C18, 0.3 ×150 mm i.d., 3 μm particle size). 10 mM ammonia acetate buffer, pH 4.0 (solvent A), and methanol + 0.1% formic acid (solvent B) were applied as mobile phase. Gradient of mobile phase was optimized to separate 8-oxodG and adducts from four DNA nucleobases. The gradient was shown in table S1. The tandem mass spectrometry method was optimized with infusion of nucleobases standards to get the maximum intensities. Multiple reaction monitoring (MRM) mode of tandem mass spectrometry method was used to quantitatively measure the amount of 8-oxodG. The ionization source was positive electrospray. The method was validated by mixing dG standard with 8-oxodG standard (10 μM each), followed by UPLC−MS/MS detection in multiple reaction monitoring (MRM) mode. Calibration curve of 8-oxodG/dG vs. MS peak area were made by making a series of solution by mixing dG and 8-oxodG standards, and measured by UPLC-MS/MS method.

Table S1. Mobile phase gradient on DNA oxidation analysis.

Time	Flow Rate (μL/min)	B%
0	6	5
1	6	5
5	6	20
6.5	6	30
8	6	30
8.5	6	5
10	6	5

UPLC−MS/MS measurement of reactive metabolites.

Fifty micrograms of rat live microsomal protein (RLM, 20 mg mL^{-1} in 250 mM sucrose) were incubated with 1 mM E_2, NADPH regenerating system, 2 mM ascorbic acid and pH 7 Tris buffer in a total volume of 500 μL for 30 min at 37 ºC. Ascorbic acid protects E_2 metabolites from oxidative degradation without affecting the metabolic enzyme activity.[2] Reaction was terminated by extracting the metabolites by 1 mL ethyl acetate twice.[3] Extracts were combined, evaporated under vacuum, and reconstituted in 200 μL acetonitrile-water (20:80). Metabolites were filtered by Omega™ membrane 96-well filtration plate (3KDa MW cutoff) and then subjected to LC-MS/MS analysis.

The metabolites were determined using a Dionex Ultimate 3000 UHPLC (Thermo Scientific, Dionex, Sunnyvale, California, USA) coupling with Applied Biosystems 4000 QTRAP mass spectrometer (AB Sciex, Foster City, CA) with a Turbo IonSpray ionization source in negative mode. 10 μL of metabolites solution was injected into a C18 (Luna, 0.5 × 150 mm, 5 μm; Phenomenex) analytical column with mobile phase A water and B acetonitrile in the gradient mode at flow rate of 10 μL min^{-1}. The gradient for sample separation is shown in table S2.

Multiple reactions monitoring (MRM) was conducted at -4500 V ion spray voltage, 300 °C, -40 V declustering potential, -55 eV collision energy, and 0.15 s dwell time for each mass transitions: E_2 (271→145), hydroxylestradiol (287→147). Enhanced product ion scanning (EPI) was performed with -55 eV collision energy for E_2 precursor ion m/z 271 (figure 6b) and hydroxylestradiol precursor ion m/z 287 (figure 6c).

Table S2. Mobile phase gradient on metabolites analysis.

Time	Flow Rate (μL/min)	B%
0	10	40
1	10	40
2	10	40
6	10	80
8	10	80
8.5	10	40
10	10	40

Results

Film construction and characterization.

Adsorbed mass/area (M/A) of each deposited, dried polyion layer was converted from the QCM resonator frequency change (ΔF) using the Sauerbrey equation:[4] M/A (g cm^{-2}) = - F (Hz)/(1.83×10^8). Where A is the area of the gold disk on the quartz resonator. Electrode area of an array electrode is 3.85×10^{-3} cm^2. Nominal thickness (d) of deposited films on the resonator was given by: [5] d (nm) = -2(0.016 ± 0.002) Δ F (Hz).

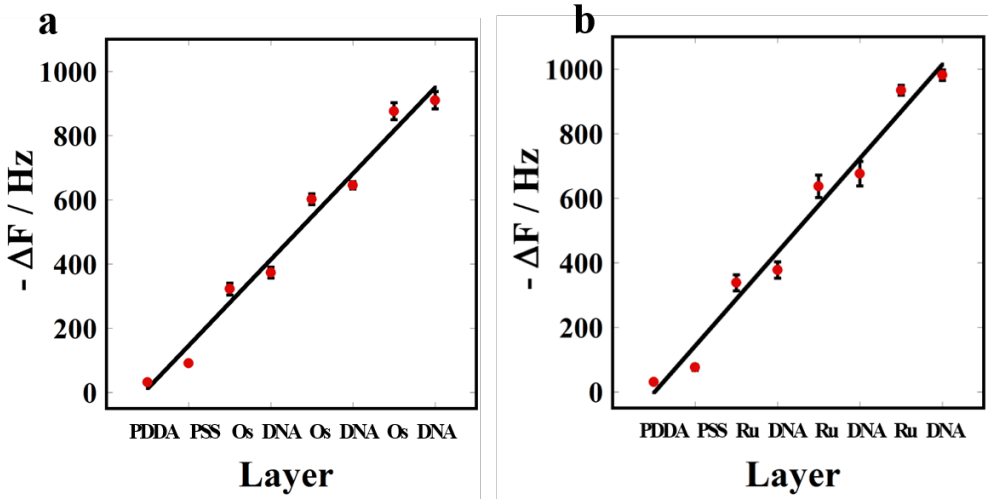

Figure S1. QCM frequency shifts for adsorption layers of (a) PDDA/PSS/$(OsPVP/DNA)_3$ and (b) (a) PDDA/PSS/$(RuPVP/DNA)_3$. (Average values from three resonators are shown with error bars. Some bars may be too small to be visible.)

Table S2. Film containing DNA/metallopolymer characteristics from QCM.

	Amount ($\mu g/cm^2$)	Nominal thickness (nm)		Amount ($\mu g/cm^2$)	Nominal thickness (nm)
PDDA	0.18 ± 0.01	1.03 ± 0.02	PDDA	0.17 ± 0.01	0.99 ± 0.06
PSS	0.32 ± 0.02	1.88 ± 0.11	PSS	0.25 ± 0.04	1.44 ± 0.24
DNA	0.70 ± 0.08	4.13 ± 0.39	DNA	0.69 ± 0.05	4.02 ± 0.13
Os	3.77 ± 0.32	22.08 ± 0.53	Ru	4.26 ± 0.31	24.94 ± 0.32
Total	4.97 ± 0.43	29.12 ± 1.05	Total	5.36 ± 0.41	31.39 ± 0.75

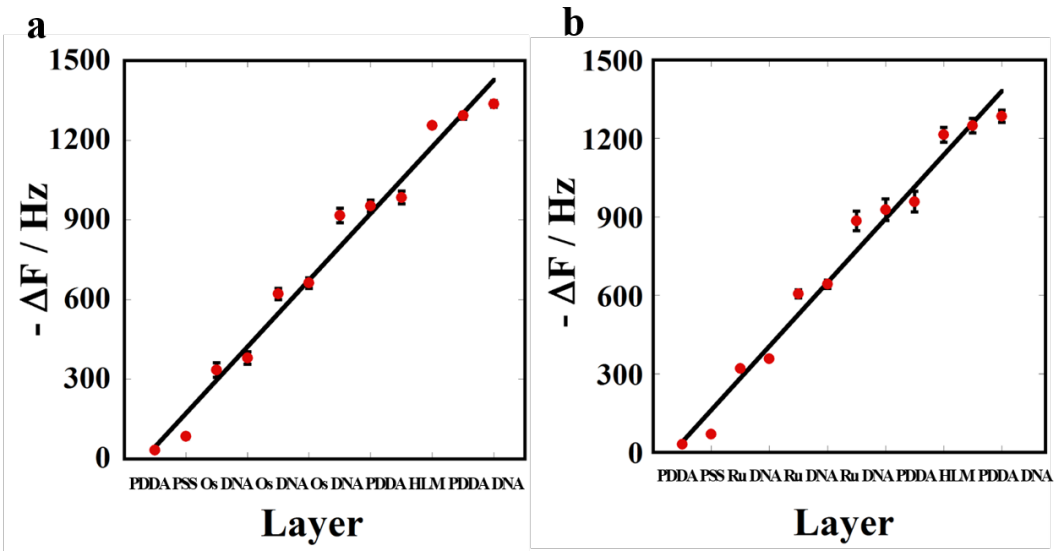

Figure S2. QCM frequency shifts for adsorption layers of (a) PDDA/PSS/$(OsPVP/DNA)_3$/PDDA/HLM/PDDA/DNA and (b) PDDA/PSS/$(RuPVP/DNA)_3$/PDDA/HLM/PDDA/DNA. (Average values from three resonators are shown with error bars. Some bars may be too small to be visible.)

Table S3. Film containing DNA/HLM/metallopolymer characteristics from QCM.

	Amount ($\mu g/cm^2$)	Nominal thickness (nm)		Amount ($\mu g/cm^2$)	Nominal thickness (nm)
PDDA	0.59 ± 0.04	3.25 ± 0.07	PDDA	0.53 ± 0.03	3.09 ± 0.07
PSS	0.28 ± 0.04	1.66 ± 0.24	PSS	0.21 ± 0.03	1.25 ± 0.15
DNA	0.91 ± 0.09	5.32 ± 0.34	DNA	0.84 ± 0.06	4.91 ± 0.07
Os	4.07 ± 0.22	23.9 ± 0.83	Ru	4.05 ± 0.23	23.70 ± 1.28
HLM	1.48 ± 0.14	8.68 ± 0.83	HLM	1.39 ± 0.09	8.16 ± 0.50
Total	7.34 ± 0.54	42.8 ± 2.31	Total	7.02 ± 0.44	41.11 ± 2.07

Detection of catechol-induced DNA oxidative damage on electrochemical array.

Catechol is a common pollutant associated with common anthropogenic activities, such as incomplete combustion of fossil fuels.[6] It generates ROS during redox cycling to produce DNA oxidative products.[7]

The arrays were exposed to 0.1 mM catechol in the present of 0.5 mM Cu^{2+} and NADPH regenerating system to generate ROS which oxidized DNA on the surface of sensor element. The ratio of the SWV difference peak current of OsPVP after the reaction ($I_{p,f}$) to that of controls with no reaction ($I_{p,i}$) was used to indicate DNA oxidative damage.[7, 8] and the SWV peak ratio ($I_{p,f}$ / $I_{p,i}$) *vs.* reaction time was depicted as Figure S3b, c. The DNA thin film underwent catechol-induced oxidative damage gave Os SWV peak current increases, whereas no significant response was found for the controls with no reaction. (Figure S3a. b) This consisted with the mechanism that after the $Os^{II}PVP$ in the sensor film was electrochemically oxidized into $Os^{III}PVP$, the $Os^{III}PVP$ could selectively catalytic oxidize 8-oxodG on DNA. [9] Longer periods of reaction time produced greater SWV peak ratio ($I_{p,f}$ / $I_{p,i}$). (Figure S3b) It suggested the increase of the extent of DNA oxidative damage with longer oxidation time, due to greater amount of 8-oxodG was formed in the DNA thin film.

Whereas for the electrodes coated with RuPVP/DNA film, the SWV difference peak current of RuPVP after the reaction ($I_{p,f}$) did not show significant response compared with that of controls with no reaction ($I_{p,i}$). The Ru SWV peak ratios ($I_{p,f}$ / $I_{p,i}$) were all close to 1 for different reaction time intervals, suggested that little DNA adducts were formed by exposing DNA with catechol.

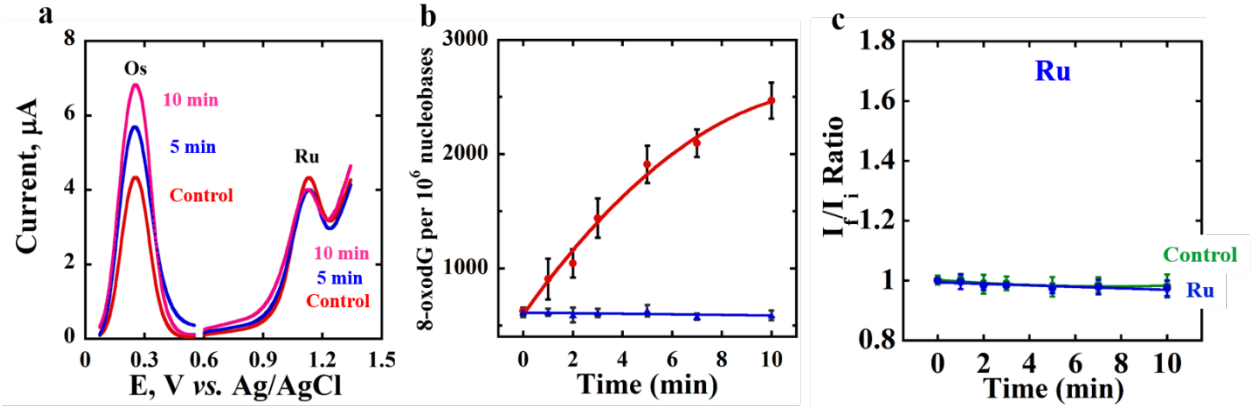

Figure S3. Difference SWVs at different reaction times in pH 5.5 buffer after incubating with 0.1 mM catechol, 0.5 mM $CuCl_2$, NADPH regenerating system for microfluidic array sensors featuring films of (a) PDDA/PSS/(OsPVP/DNA)$_3$ and PDDA/PSS/(RuPVP/DNA)$_3$ (SWV ampl., 25 mV; freq., 15 Hz; step, 4 mV). (b) Influence of reaction time on SWV peak current ratio ($I_{p,f}/I_{p,i}$) of PDDA/PSS/(OsPVP/DNA)$_3$ and PDDA/PSS/(RuPVP/DNA)$_3$ films for the same reaction with catechol. Controls are array incubated in the same mixture absence of catechol. (Error bars represent standard deviations for n= 4.)

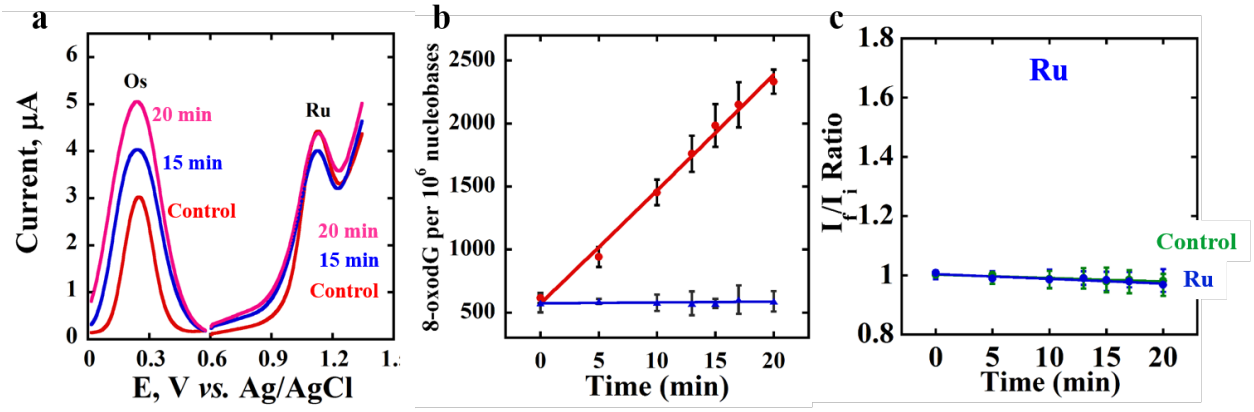

Figure S4. Difference SWVs at different reaction times in pH 5.5 buffer after incubating with 2.5 mM 2-NO-T, 0.5 mM $CuCl_2$, NADPH regenerating system for microfluidic array sensors featuring films of (a) PDDA/PSS/(OsPVP/DNA)$_3$ and PDDA/PSS/(RuPVP/DNA)$_3$ (SWV ampl., 25 mV; freq., 15 Hz; step, 4 mV). (b) Influence of reaction time on SWV peak current ratio ($I_{p,f}/I_{p,i}$) of PDDA/PSS/(OsPVP/DNA)$_3$ and PDDA/PSS/(RuPVP/DNA)$_3$ films for the same reaction with 2-NO-T. Controls are array incubated in the same mixture absence of 2-NO-T. (Error bars represent standard deviations for n= 4.)

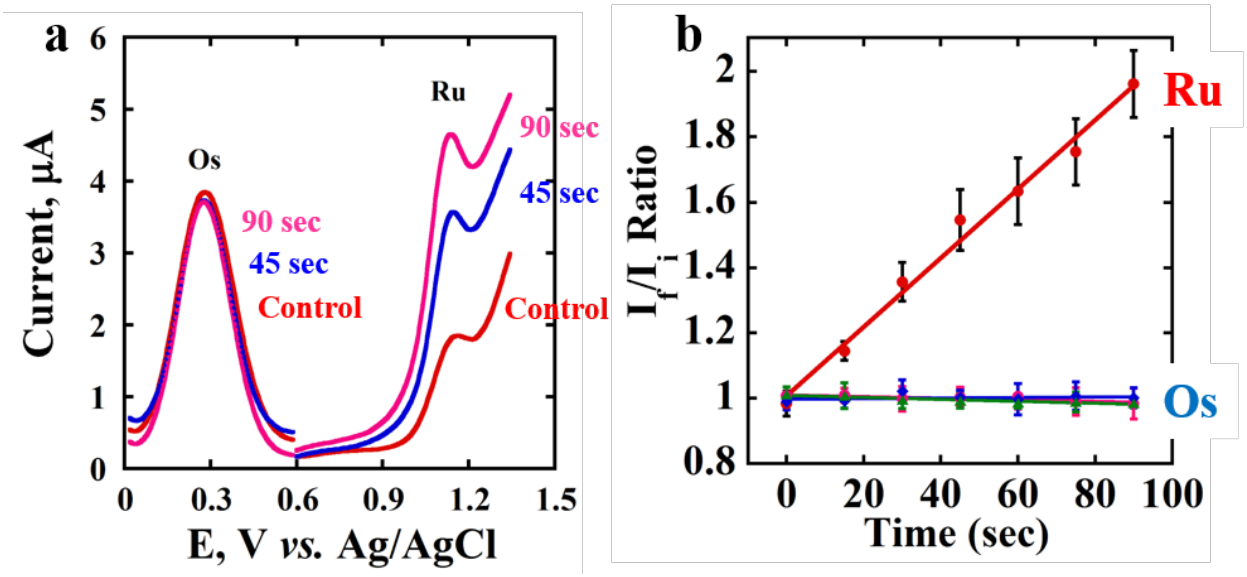

Figure S5. Difference SWVs at different reaction times in acetate buffer after incubating with 250 µM 2-AAF, 0.5 mM $CuCl_2$, NADPH regenerating system for microfluidic array sensors featuring films of (a) PDDA/PSS/$(RuPVP/DNA)_3$/PDDA/HLM/PDDA/DNA and PDDA/PSS/$(OsPVP/DNA)_3$/PDDA/HLM/PDDA/DNA (SWV ampl., 25 mV; freq., 15 Hz; step, 4 mV). (b) Influence of substrate incubation time on SWV peak current ratio ($I_{p,f}/I_{p,i}$) for the same sensors reacted with 2-AAF. Controls are incubations in the absence of 2-AAF. (Error bars represent standard deviations for n= 4.)

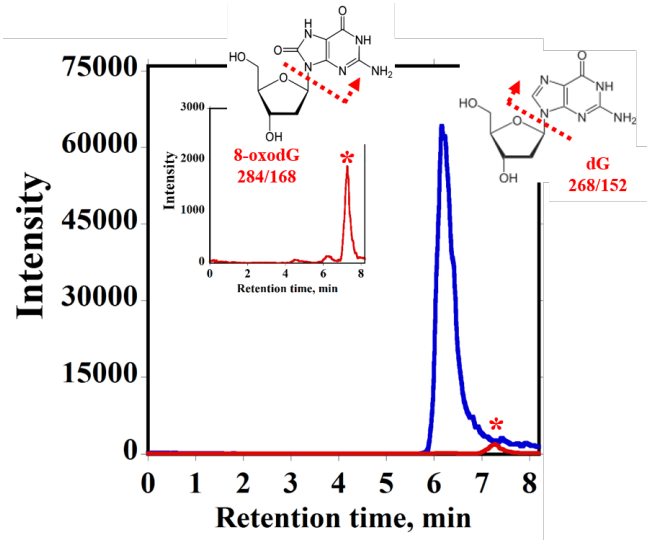

Figure S6. HPLC−MS/MS results: HPLC-MS/MS chromatogram in MRM mode obtained for the ions at m/z 268→152 transition (dG) and 284 →168 transition (8-oxodG, inset) for DNA magnetic biocolloid reactors reacted with 0.5 mM 4-OHE_2 with 0.5 mM Cu^{2+} and NADPH regenerating system for 10 time.

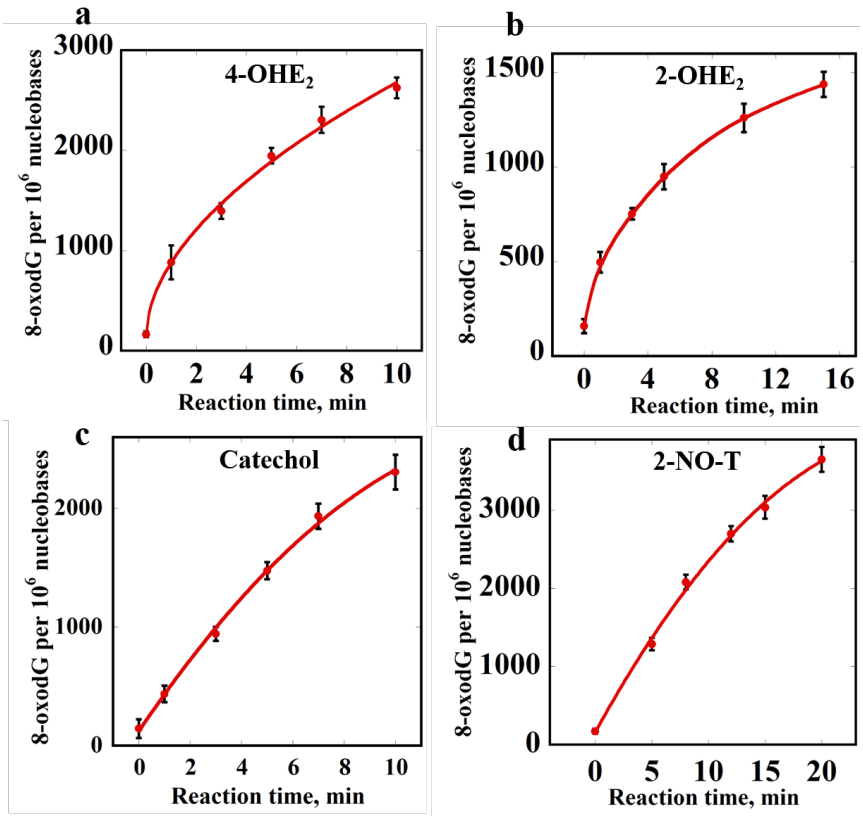

Figure S7. Number of 8-oxodG per 10^6 nucleobases from the magnetic biocolloid reactors reacted with (a) 0.5 mM 4-OHE_2, (b)0.5 mM 2-OHE_2, (c)0.1 mM catechol, (d) 2.5 mM 2-NO-T in the present of 0.5 mM Cu^{2+} and NADPH regenerating system for different time and then hydrolyzed. (Error bars represent standard deviations for three different measurements.)

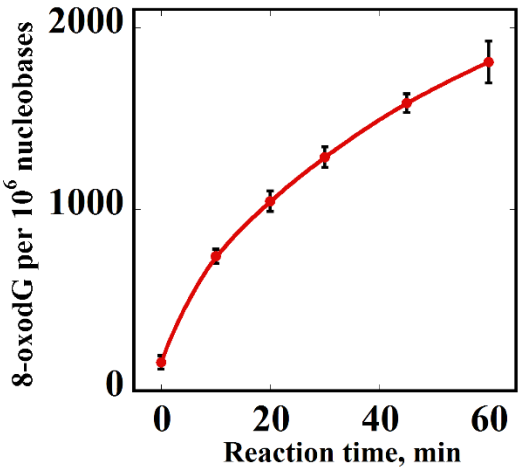

Figure S8. Number of 8-oxodG per 10^6 nucleobases from the magnetic biocolloid reactors reacted with E_2 metabolites in the present of 0.5 mM Cu^{2+} and NADPH regenerating system for different time and then hydrolyzed. (Error bars represent standard deviations for three different measurements.)

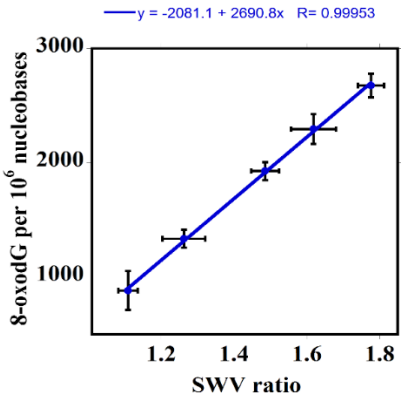

Figure S9. Calibration curve for sensor SWV current ratio *vs.* relative amount of 8-oxodG in DNA on the array reacted with 4-OHE_2. (Error bars represent standard deviations for three measurements.)

References

[1] C. L. Hayes, D. C. Spink, B. C. Spink, J. Q. Cao, N. J. Walker and T. R. Sutter, *Proc. Natl Acad. Sci. USA*, 1996, **93**, 9776-9781.
2 A. F. Badawi, E. L. Cavalieri and E. G. Rogan, *Carcinogenesis*, 2000, **21**, 1593-1599.
3 C. L. Hayes, D. C. Spink, B. C. Spink, J. Q. Cao, N. J. Walker and T. R. Sutter, *Proc. Natl Acad. Sci. USA*, 1996, **93**, 9776-9781.
4 Y. M. Lvov, Z. Lu, J. B. Schenkman, X. Zu and J. F. Rusling, *J. Am. Chem. Soc.*, 1998, **120**, 4073-4080.
5 Y. Lvov and R. W. Nalwa, in *Handbook of Surfaces and Interfaces of Materials*, ed. Academic Press, San Diego, CA, **2001**, Vol. 3, pp 170-189.
6 A. Pawar, S. Ugale, M. More, N. Kokani and S. Khandelwal, *J. Bioremed. Biodeg.* 2013, **4**, 203.
7 B. Song, S. Pan, C. Tang, D. Li and J. F. Rusling, *Anal. Chem.*, 2013, **85**, 11061-11067.
8 A. Mugweru, B. Wang and J. Rusling, *Anal. Chem.*, 2004, **76**, 5557-5563.
9 (1) A. Mugweru and J. Rusling, *Electrochem. Commun.* 2001, **3**, 406−409. (2) A. Mugweru, B. Wang and J. Rusling, *Anal. Chem.,* 2004, **76**, 5557-5563. (3) J. F. Rusling, in *Perspectives in Bioanalysis*, eds. F. S. Emil Paleček and J. Wang, Elsevier, **2005**, vol. Volume 1, pp. 433-450.